

Synthesis of Poly(methyl methacrylate)/Silica Nanocomposite Through Emulsion Polymerization Using Dimethylaminoethyl Methacrylate

Mohammad Barari, Naser Sharifi-Sanjani

School of Chemistry, University College of Science, University of Tehran, Tehran, Iran

Received 22 November 2007; accepted 29 April 2008

DOI 10.1002/app.28706

Published online 10 July 2008 in Wiley InterScience (www.interscience.wiley.com).

ABSTRACT: Polymer/Silica nanocomposite latex particles were prepared by emulsion polymerization of methyl methacrylate (MMA) with dimethylaminoethyl methacrylate (DM). The reaction was performed using a nonionic surfactant and in the presence of silica nanoparticles as the seed. The polymer-coated silica nanoparticles with polymer content and number average particle sizes ranged from 32 to 93 wt % and 114–310 nm, respectively, were obtained depending on reaction conditions. Influences of some synthetic conditions such as MMA, DM, surfactant concentration, and the nature of initiator on the coating of the silica nanoparticles were studied. Electrostatic attraction between anionic surface of silica beads and cationic amino groups of DM is the main driving force for the formation of the nanocomposites. It was

demonstrated that the ratio of DM/MMA is important factor in stability of the system. The particle size, polymer content, efficiency of the coating reaction, and morphology of resulted nanocomposite particles showed a dependence on the amount of the surfactant. Zeta potential measurements confirmed that the DM was located at the surface of the nanocomposites particles. Thermogravimetric analysis indicated a relationship between the composition of polymer shell and polymer content of the nanocomposites. The nanocomposites were also characterized by FTIR and differential scanning calorimetry techniques. © 2008 Wiley Periodicals, Inc. *J Appl Polym Sci* 110: 929–937, 2008

Key words: emulsion polymerization; nanocomposites

INTRODUCTION

In the past few years, organic/inorganic nanocomposite particles have become the subject of rapidly growing interest for their superior properties such as optical, mechanical, rheological, catalytic, and fire retardancy. Their extraordinary properties derived from the synergism of the properties of inorganic particles (such as mechanical strength, modulus, and thermal stability) along with the processability and flexibility of organic polymer matrix. Such materials can be obtained as colloidal suspension by heterophase polymerization. Examples of preparation of organic–inorganic nanostructured colloids via suspension,¹ dispersion,^{2,3} miniemulsion,^{4–6} and emulsion polymerization can be found in the literatures. Among the techniques, seeded emulsion polymerization is the most frequently used one. By this technique, nanocomposite particles with a variety of morphology and structure were obtained. However, for successful preparation of the nanocomposites, there must be created a good compatibility between

hydrophilic inorganic particles and hydrophobic polymers. So, it is necessary to use some interfacial promoters to create specific interaction and increase interfacial adhesion between the moieties. Pretreatment of an inorganic compound with coupling agent bearing polymerizable double bond is one approach to promote compatibility between the phases. For example, Zhang et al. reported the pretreatment of silica particles using trimethoxy silyl (propyl methacrylate) followed by emulsion polymerization of styrene.⁷ In this work, silica/polystyrene composite particles with core-shell morphology were obtained through encapsulating the surface of modified silica particles by polystyrene. Reculosa et al. prepared micrometer polystyrene/silica particles by using adsorbed poly (ethyleneglycol methacrylate) to enhance adhesion between the polystyrene particles and the silica surface.⁸

Surface charge attraction can also be used as the driving force for encapsulation reactions. Such interactions, modulated by pH, have been reported by several authors. For instance, Haga et al. described the PMMA encapsulation reaction of titanium dioxide using initiators with a charge opposite to the surface charge of the pigment.⁹ Similarly Bourgeat-Lami and coworkers, described the preparation of

Correspondence to: M. Barari (barari@khayam.ut.ac.ir).

poly(methyl methacrylate)/silica nanocomposite particles using an electrostatically adsorbed cationic initiator to promote polymerization at the surface of an anionic silica sol.^{10,11} Another similar approach is using auxiliary monomer to strongly adsorb onto inorganic surface and promote strong interfacial interaction between the organic polymer and the inorganic phase. Armes and coworkers, proposed a method to synthesize a series of raspberry-like core-shell nanocomposite particles with vinyl polymer as core and nanosilica as shell.¹²⁻¹⁷ In their method 4-vinylpyridine (4VP) was used as an auxiliary monomer. The basic property of the amino groups from 4VP could interact with the acidic property of the hydroxyl groups from nanosilica surface to enhance compatibility between the organic phase and the inorganic phase. Wu and coworkers, subsequently used 1-vinylimidazole (1VID) as the auxiliary monomer and synthesized long stable raspberry-like PMMA/silica nanocomposite particles.¹⁸ Using this synthetic route makes free from the necessity of pretreatment of surface silica and the composite is prepared in one pot synthetic procedure.

Herein, we report the synthesis of poly(methyl methacrylate)/silica nanocomposite via emulsion polymerization of methyl methacrylate (MMA) using dimethylaminoethyl methacrylate (DM) as auxiliary monomer. To the best of our knowledge, the use of this auxiliary monomer for preparation of the nanocomposites has not been reported yet. In this method, two-layer hybrid structures with silica beads as inorganic core, and poly(methyl methacrylate) as shell, was formed. Some influencing parameters in the formation of the nanocomposite particles such as MMA, DM, surfactant amount, and nature of initiator were investigated in detail.

EXPERIMENTAL

Materials

Methyl methacrylate (MMA, Merck, $\geq 99\%$) was purified via treating with aqueous NaOH (5%) to remove inhibitor and dried over by anhydrous CaCl_2 then stored at low temperature prior to use. (2-dimethylaminoethyl) methacrylate (DM, Merck, $\geq 99\%$) was purified by distillation under reduced pressure before use. The nonionic polyoxyethylene octylphenol surfactant with average number of ethylene oxide units of 40 (TX-405, Aldrich, 70% solution in water) and the initiators 2,2'-Azobis(isobutyramidine) dihydrochloride (AIBA, Acros, $\geq 98\%$) and Ammonium persulfate (APS, Merck, $\geq 98\%$) were used as received. The colloidal silica nanoparticles with intensity average diameter of 103 ± 13 nm were synthesized using so-called Stöber method.¹⁹

TABLE I
Recipe for Synthesis of Nanocomposite Particles

Ingredient	Amount (g)	Concentration (based on water)
Water	50	
Silica	0.75	1.5 wt %
MMA	5–12.5	1–2.5 mol/L
DM	0–1.24	0–0.158 mol/L
TX 405	0.11–0.59	1.12–6 mmol/L
AIBA ^a	0.05	3.7 mmol/L

^a In run 8, AIBA was replaced by an equimolar amount (0.042 g) of APS.

Nanocomposite synthesis

The polymer/silica nanocomposites were prepared by free radical emulsion polymerization of MMA with DM as comonomer in the presence of silica. The experiments were performed using the recipe presented in Table I. The typical procedure for running the experiments is as follows: The DM was added to an aqueous dispersion containing 1.5 wt % silica beads in a round bottom flask fitted with a reflux condenser and thermometer. This mixture was stirred at room temperature for 30 min before MMA and Triton X-405 were added. The emulsion mixture was degassed with nitrogen and heated to 60°C. Then, the initiator dissolved in deionized water was degassed and added into the reaction vessel. The polymerization was carried out for 24 h. As the coating reactions caused the formation of both nanocomposite and free latex particles, the nanocomposite particles were separated from the free latex particles by centrifugation-redispersion cycles from the original latex dispersion for several times with each successive supernatant being removed and replaced by deionized water.

Characterization

The monomer conversions were determined gravimetrically by measuring the solid content of the original latex. To determine the polymer content and the efficiency of the coating reaction, thermogravimetric analysis was performed with a TA Q50 instrument (TA Instruments, New Castle, De USA). The coated silica was dried at 50°C to constant weight. The dried purified powders were heated in argon to 700°C at a scan rate of 20°C/min. The polymer content purified nanocomposites and efficiency of the coating reactions were calculated as follows:

$$\text{polymer content (wt \%)} = \frac{\text{amount of polymer in the composite sample}}{\text{amount of composite sample}} \times 100 \quad (1)$$

TABLE II
Summary of Reaction Conditions for Coating Experiments and their Characterization

Run no.	MMA (mol/L)	DM (mol/L)	TX 405 (mmol/L)	Conversion of monomer (%)	Polymer content (wt %)	Efficiency (%)	Composite particle diameter (nm)		PDI ^a
							TEM	DLS ^b	
1	1	0	3.05	n.a. ^c	–	–	–	–	–
2	1	0.064	3.05	92	52	16	140	268	0.044
3	1	0.095	3.04	94	51.5	14.8	138	257	0.024
4	1.5	0.064	3.06	n.a.	–	–	–	–	–
5	1.5	0.095	3.06	89	62	16.7	170	277	0.205
6	2	0.127	3.06	90	89	61.3	283	363	0.236
7	2.5	0.158	3.05	87	93	83.2	310	484	0.237
8 ^d	1	0.064	3.06	92	49.5	14.5	135	247	0.073
9	1	0.064	1.12	93	80	58.6	205	334	0.167
10	1	0.064	2	92	69	27.5	176	288	0.066
11	1	0.064	6	94	32	6.8	114	212	0.083

^a PDI were measured using light scattering method.

^b Intensity average diameter of the composite particles as determined by dynamic light scattering studies.

^c The products are not analyzed due to the large amount of precipitated were obtained.

^d 3.7 mmol/L APS was used instead of AIBA.

Efficiency of the coating reaction (wt %)

$$= \frac{\text{amount of polymer in the composite sample}}{\text{total amount of polymer formed}} \times 100 \quad (2)$$

The infrared spectra were recorded using a Bruker EQUINOX FTIR spectrometer (Germany). Differential scanning calorimetry data were obtained using a TA Q100 instrument (TA Instruments, New Castle, De USA) between -20 and 170°C under argon purge, at heating rate of $10^{\circ}\text{C}/\text{min}$.

Intensity average particle size and zeta potential measurements were performed using a Malvern Nano-ZS instrument (Southborough, UK) and the data were processed using the Malvern DTS software version 4.2. For zeta potential measurements the solution pH was adjusted by addition of either NaOH or HCl. The morphology and number average diameter of the purified nanocomposite particles were studied by transmission electron microscopy (TEM). Diluted nanocomposite dispersions were dried onto carbon coated cooper grids and observed using a Carl Ziss CEM 902 instrument (Oberkochen, Germany) operating at 80 kV. More than hundred particle diameters were measured for each sample and used to calculate number average diameter.

RESULTS AND DISCUSSION

Influence of DM and MMA concentration

Table II summarizes the preparation of a series of nanocomposite particles obtained via emulsion polymerization. The driving force for the synthesis of

these nanoparticles is acid base interaction between surface hydroxyl groups of silica and amino functional groups of DM. To examine the influence of DM on systems, a control experiment was carried out according to the recipe given in Table II (run 1). The reaction without DM led to macroscopic precipitate with no colloid formation. In the second experiment (run 2), When 0.064 mol/L DM was included in the polymerization formulation, a stable colloidal dispersion was obtained with no precipitated particles. Polymer content of the purified nanocomposites and the efficiency of run 2 were 52 wt % and 16%, respectively. Figure 1 shows the composite particles from run 2 and bare silica for comparison. The images in Figure 1(b) reveal that the nanocomposite particles have a polymer layer with about 20 nm thickness around the silica nanoparticles. The two runs serve to illustrate the essential role played by DM in the creation of the nanocomposite particles and promoting colloid stability of the systems. For all formulations containing DM monomer listed in Table I, the stable products were formed (except run 4 that will be discussed below). The monomer conversions were relatively high and ranging from 87 to 95%. Further increase in the DM charge to 0.095 mol/L, shown in run 3, has no discernible effect on polymer content, which suggests that there is an excess of DM under these conditions. It is probable that in high DM content, more hydrophilic polymers grow by themselves to form the stable free latex particles and did not easily adsorb on the anionic silica particles because they are surrounded by their own electric double layer. It demonstrates the finite requirement for DM for stability and creation of the core-shell structure particles.

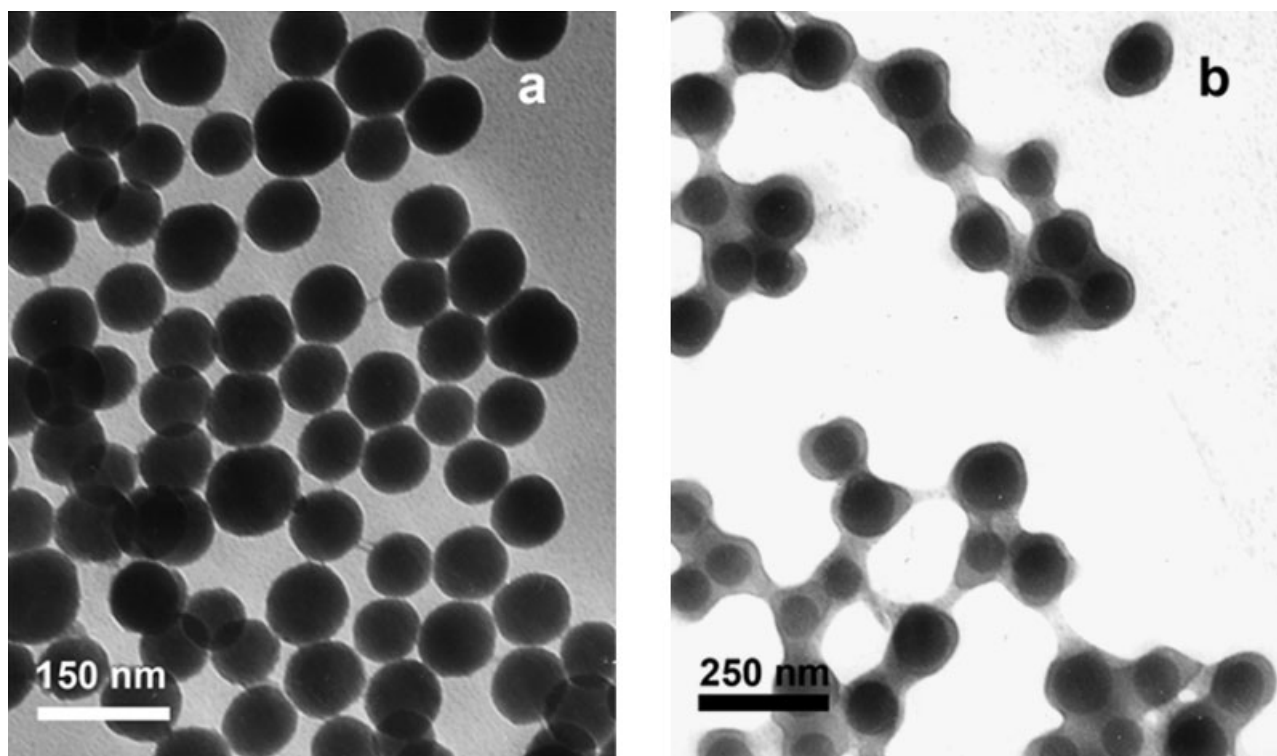


Figure 1 TEM image of (a) bare silica and (b) nanocomposite particles from run 2.

To investigate effect of MMA concentration, when the initial charge of MMA was increased to 1.5 mol/L in formulation (run 4 in Table II), mainly precipitate unstable system was obtained. TEM study of purified composite of the stable portion of the system showed that silica particles were partially covered with a few polymer particles and no encapsulation was found in the TEM image (not shown). In run 5, increasing initial amount of DM to 0.095 mol/L with the content of MMA the same as in the formulation of run 4, led to the formation of a stable system. In this reaction, the molar ratio of DM to MMA was 0.063, about the same ratio of DM/MMA in run 2. This ratio was kept constant in the recipes with higher concentration of MMA (run 6 and run 7) and resulted in stable systems. It can be said that the DM/MMA molar ratio of 0.063 is recommended for a successful synthesis of a stable system. TEM studies of the composite particles resulting from runs 5–7 showed silica particles were well coated with the polymer shell around it. Typical TEM photograph of the samples are shown in Figure 2.

Particle size and thermogravimetric studies showed that the composite particles become larger and the polymer content and the efficiency of coating reaction led to an increase with the amount of the monomer, indicating a direct relationship between the quantities and the monomer amount. It demonstrates that the polymerization and adsorp-

tion of the polymer is mainly performed on the silica surface. It is obvious that increasing amount of polymer in the composite particles mainly resulted from the amount of MMA (due to high molar ratio of MMA/DM) but it seems DM plays important role in successful synthesis of the composite in high monomer content. As the particles become larger, more stabilizers are needed to ensure the stability of growing particles. Since, the nonionic surfactant concentration was kept constant and considering the instability, resulted from insufficient DM content in run 4, one can conclude that increasing the amount of DM (keeping constant the ratio of DM/MMA) is responsible for the enhancement of stability of the composite particles in high monomer conditions. On the other hand, with decreasing proportion of the surfactant in stability of the system, the efficiency of polymer adsorption on silica becomes more significant, probably due to better performance in interaction of DM units with silica surface. This led to concomitant enhancement of polymer content and coating efficiency with monomer concentration. Similar results were also found in the experiments with low surfactant content (see below).

Influence of initiator

There are some reports about synthesis of nanocomposite particles in which AIBA has a main role in interaction between polymer and the mineral

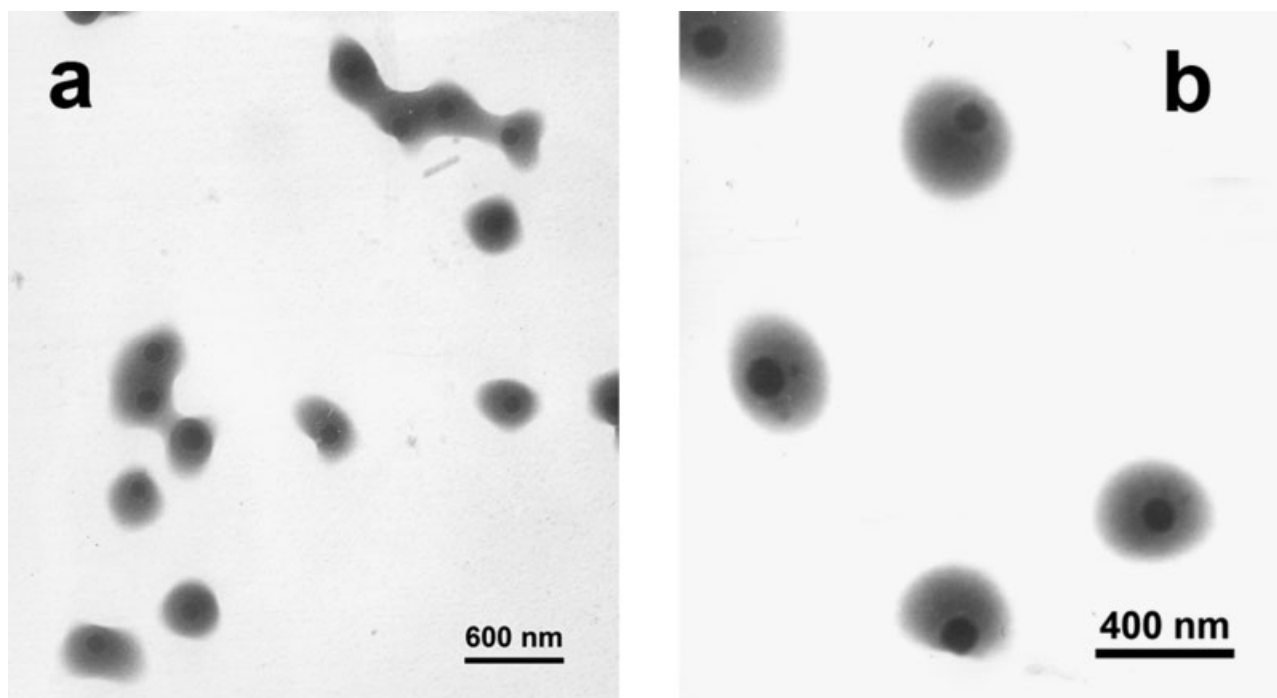


Figure 2 TEM images of composite particles resulting from (a) run 6 and (b) run 7.

moieties.^{10,11} To investigate the contributions of initiator on the coating reaction in our systems, an anionic initiator, APS, was used (run 8) instead of the cationic initiator. The anionic initiator was selected because it does not participate in coating reaction due to the same charge of the surface of silica and APS. The anionic initiator used equimolar amount of AIBA. The other conditions were the same as those of run 2. Measurement of polymer content of the composite particles from run 8, is 49.5 wt %, almost the same as the result of run 2. This experiment indicated that the role of AIBA is minor in our reaction and the interaction between the polymer shell and silica surface is mainly affected by the cationic monomer.

Influence of surfactant concentration

In some previous works on encapsulation of silica, it has been shown that surfactant is an important factor in the coating reaction of silica.^{20,21} To illustrate the importance role of surfactant in our experiments, a series of control experiments with various content of DM were performed in the absence of TX 405 (not listed). In none of the control experiments, stable dispersions were obtained. These results indicated that the existence of an adequate amount of surfactant to be adsorbed on the surface of growing particles is essential to carry out the coating reaction in stable state.

To investigate the effect of the amount of the surfactant, a series of coating reactions with different concentration of TX 405 were performed. The evolu-

tion of particle size, polymer content and the efficiency of coating, as a function of the surfactant content were investigated (Table II, runs 2, 9–11). Increasing the surfactant in the feed led to a decrease in the particle size, polymer content, and coating efficiency. It is probably, in excess TX 405 concentration, the surfactant molecules promote the stability of the oligomer generated in aqueous phase before they are adsorbed on the surface of silica particles and hence cause the undesirable generation of free lattices to become noticeable. It can be anticipated that the free lattices will be preferred to adsorb further monomer and/or oligomer and will thus become the main locus of polymerization, the secondary nucleation process which will obviously contribute to a decrease in particle size, coating efficiency and polymer content. In the case of smaller surfactant amount in contrast, the attraction of the monomer and/or forming polymer on the silica particles is rather important and more polymer builds up at the inorganic surface.

TEM studies of the composite particles (Fig. 3) showed that at high concentration of the surfactant, only a uniform thin polymeric layer covers the silica particles. The polymeric shell becomes thicker and more irregular in shape with lowering amount of the surfactant. For the run with the lowest surfactant content, the shape of the particles has a raspberry-like morphology as shown in Figure 3. A smooth coating would suggest the growth of polymer shell is limited by the nucleation of the forming polymers

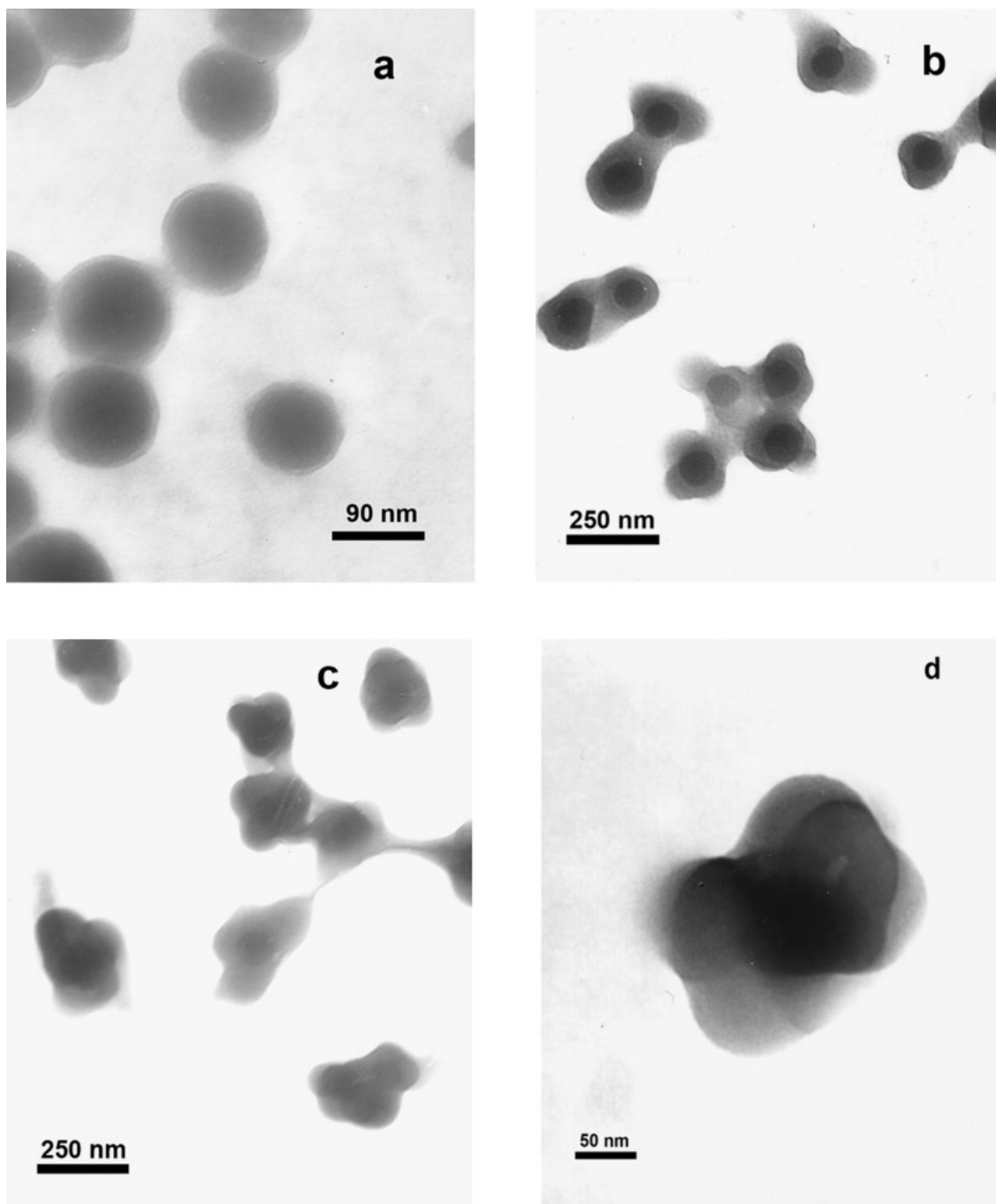


Figure 3 TEM micrographs of composite particles (a) run 11, (b) run 10 and (c,d) run 9.

on the silica surface, while a raspberry-like structure would point to homogenous nucleation of the bulk, accompanied by the attachment of the polymer particles to SiO_2 surface, becomes dominant due to the deficient stabilization of the surface of the particles.

FTIR analysis

The composite products were characterized by FTIR spectroscopy. Figure 4 shows typical FTIR spectra of the composites. The spectra in Figure 4 confirm that

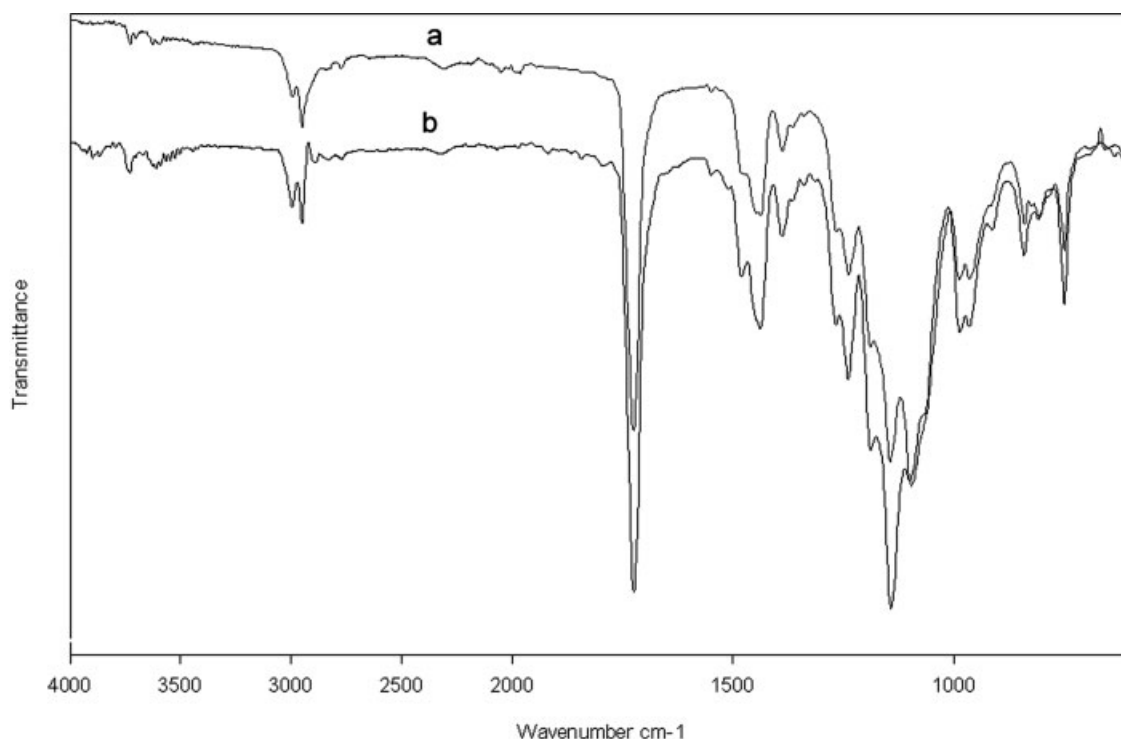


Figure 4 FTIR spectra of selected composite samples: (a) run 10 and (b) run 7.

the particles are composed of silica and the polymer based on the presence of vibration bands at around 1100 cm^{-1} attributed to arising from Si—O—Si stretching modes of silica and a band at 1727 cm^{-1} corresponding to C=O vibration of the polymer. The two signals at 2993 and 2949 cm^{-1} are related to CH_3 and CH_2 stretching vibration of methacrylate units. The weak bands are observed at 2830 and 2790 cm^{-1} which is attributed to CH_3 and CH_2 stretching of amino pendant groups of DM units. The remaining signals of DM overlap with vibration bands of the MMA and there is no discernible difference between the two monomeric units at the other vibration bands.

Particle size analysis

The average particle sizes of composite particles measured by DLS and TEM are given in Table II. DLS measurement provides an intensity average diameter which is sensitive to the presence of larger particles. It is worth noting that the diameter of composite latex particles determined by DLS is larger than that determined by TEM. The difference indicates an aggregation which is most probably due to experimental parameters used for the separation of the free lattices in centrifugation process.²² In all products, the original samples were stable for several months with no aggregation but purified samples were flocculating in a few days.

Surface potential measurement

The zeta potential of the composite particle from run 2 was recorded as a function of pH. The results shown in Figure 5 indicate that at low pH, the zeta potential is positive and decreases with an increase in pH. At low pH, DM is protonated and hence it has cationic characteristic which results in positive zeta potential. With increasing pH, DM is deprotonated and the zeta potential decreases, and at $\text{pH} = 10$, it become negative. The negative charge probably originates due to the hydrolysis of amidine function (resulted from AIBA) into carboxylic acid under alkaline conditions.^{23,24} This observation is an evidence for the presence of the basic DM residues which did not interact with the silica surface and were located

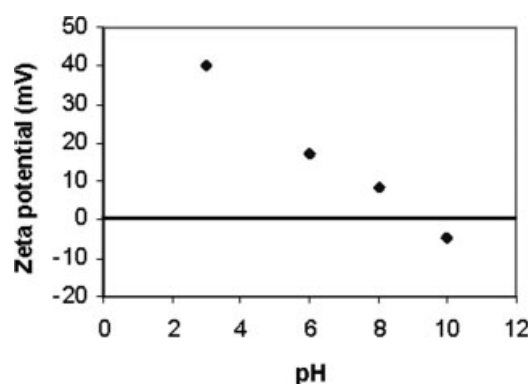


Figure 5 Zeta potential versus pH curve for nanocomposite particles from run 2.

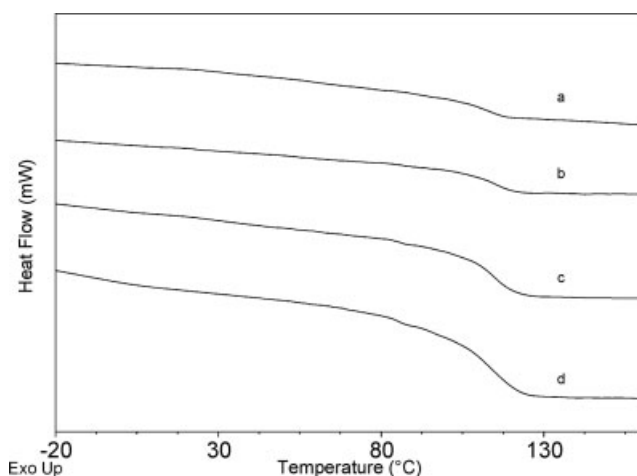


Figure 6 DSC curves for the composite particles obtained from (a) run 2, (b) run 10, (c) run 6, and (d) run 7.

at the surface of the composite particles owing to high water solubility of DM comonomer. This gives the surface of the particles a basic character of which the charge varies with the pH of medium.

Thermal analyses

Differential scanning calorimetry studies were performed on the polymer/silica composite formulation of run 2, 6, 7, and run 10. The glass transition temperature, T_g , of a polymer corresponds to the onset of significant segmental chain motion. The results presented in Figure 6 show a T_g at $\sim 114^\circ\text{C}$ which is attributed to glass transition of poly(methyl methacrylate) which remains unaffected by the inorganic part of the composite. Enthalpy change of the samples varies with the polymer content of the nanocomposite. This runs in accordance with a number of reports concerning polymer-based composites, the

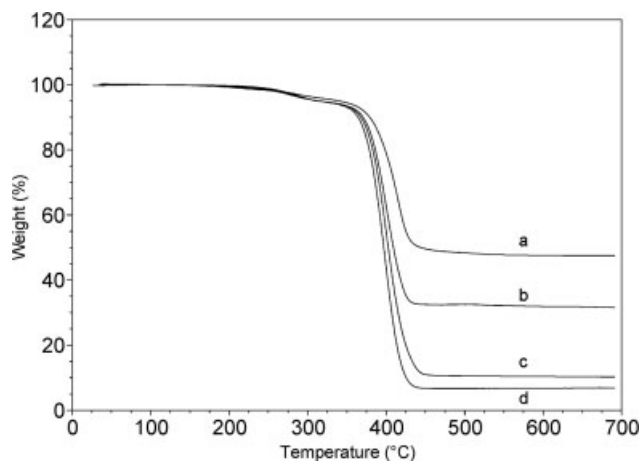


Figure 7 Thermogravimetric degradation curves for the composite particles obtained from (a) run 2, (b) run 10, (c) run 6, and (d) run 7.

TABLE III
Percentage of the First Weight Loss from Polymer Shell of Nanocomposites During Thermogravimetric Analysis

Run no.	Weight loss of first transition 175–330°C (wt %)	calculated DM content (wt %) ^a
2	4.03	16.8
3	4.22	17.9
5	4.6	16.4
6	4.8	11.7
7	5.1	11.9
8	4.45	19.6
9	4.84	13.2
10	5.2	16.5
11	5.3	35.7

$$^a \text{DM content (wt\%)} = \frac{\text{Weight loss of first transition}}{0.46 \times \text{PC}} \times 100.$$

change in specific heat observed at the T_g of the organic phase usually reduces relative to polymer content of the system.²⁵ For the composite from run 6 and 7, a barely discernable T_g are observed at $\sim 86^\circ\text{C}$ which may be related to copolymer chains with higher DM monomeric units. The absence of clear T_g in this region may be attributed to confinement of the polymer chain due to polymer/silica interaction. This region is more obvious in the system where the higher polymer content implies more freedom of movement for chain segments of the copolymers.

Thermogravimetric (TGA) analysis was used to characterize the nanocomposites and assess thermal degradation behavior of the polymer shell of the samples. The typical TGA degradation for the nanocomposites is shown in Figure 7. The weight loss found in the first major transition is possibly due to loss of vinylamine fragment through the cleavage of the dimethylaminoethyl side chain. The weight loss during the second transition may occur via cleavage of the remnants of the DM side chains and the

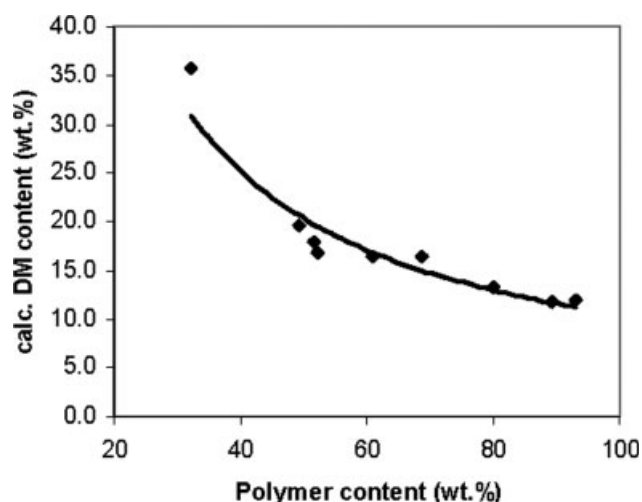


Figure 8 Relationship between the calculated DM content and polymer content.

degradation of MMA chains by radical unzipping.^{26,27} Theoretical mass loss of dimethyl aminoethyl group from one DM unit is about 46 wt %. Taking of this theoretical mass loss into account, DM content of the polymer shell can be calculated from the first weight loss of TGA thermograms. The calculated weight ratios of DM to total polymer in the coated particles are listed in Table III. The study of variation of the proportion of calculated DM content in comparison to that of polymer content of the composite particles (Fig. 8) indicated that in the particle with low polymer content the silica surface was selectively coated with limited amount of DM rich copolymers which have a better interaction with silica. At higher polymer content, DM content decreases and reaches about the DM feed content indicating higher proportion of less hydrophilic polymer in the polymer shell.

CONCLUSIONS

In this work, water borne colloidal silica/polymer nanocomposites were successfully prepared via emulsion polymerization of MMA and auxiliary comonomer DM. The polymerization was performed in the presence of silica and TX 405 as nonionic surfactant. Electrostatic interaction of DM with the surface of silica nanoparticles ensures the coating reaction. Addition of sufficient amount of DM gives stable nanocomposite systems. In high monomer feed conditions, a constant DM/MMA ratio is found to obtain stable systems with high particle size, polymer content, and efficiency. In our reaction conditions, cationic initiator has a minor effect on the coating reaction. The nonionic surfactant has an essential role in the stability of the composite systems, and influences polymer content, efficiency, size and morphology of final nanocomposites. Zeta potential measurement showed the presence of cationic DM groups on the surface of the composite particles. DSC thermograms indicate a discernable glass transition assigned to poly(methyl methacrylate) and less discernable glass transition related to the copolymers that is probably impeded by interaction of the silica surface. TGA studies confirm the presence of DM units in polymer shell of composite particles and its amount varies with polymer content. The advantage of our system is that it enables us to form nanocomposites particles in only one step without any pretreatment of silica surface, and with the use of the conventional ingredients of emulsion polymerization systems. However, in this method, formation of the free latex particles are unavoidable, thus centrifugation is required here to separate the composite particles. This method is potential interest

in other inorganic nanoparticle coating for various applications such as paint formulation.

The authors express their special gratitude to Mr. Hashemi for obtaining TEM micrographs in the laboratory of electronic microscopy of University College of Science in the University of Tehran.

References

1. Duguet, E.; Abboud, M.; Morvan, F.; Maheu, P.; Fontanille, M. *Macromol Symp* 2000, 151, 365.
2. Bourgeat-Lami, E.; Lang, J. *J Colloid Interface Sci* 1998, 197, 293.
3. Bourgeat-Lami, E.; Lang, J. *J Colloid Interface Sci* 1999, 210, 281.
4. Tiarks, F.; Landfester, K.; Antonietti, M. *Langmuir* 2001, 17, 5775.
5. Erdem, B.; Sudol, E. D.; Dimonie, V. L.; El-Aasser, M. *J Polym Sci Part A: Polym Chem* 2000, 38, 4419.
6. Faridi-Majidi, R.; Sharifi-Sanjani, N. *J Appl Polym Sci* 2007, 105, 1244.
7. Zhang, K.; Chen, H. T.; Chen, X.; Chen, Z. M.; Cui, Z. C.; Yang, B. *Macromol Mater Eng* 2003, 288, 380.
8. Reculusa, S.; Poncet-Legrand, C.; Ravaine, S.; Mingotaud, C.; Duguet, E.; Bourgeat-Lami, E. *Chem Mater* 2002, 14, 2354.
9. Haga, Y.; Watanabe, T.; Yosomiya, R. *Angew Makromol Chem* 1991, 189, 23.
10. Luna-Xavier, J. L.; Bourgeat-Lami, E.; Guyot, A. *Colloid Polym Sci* 2001, 279, 947.
11. Luna-Xavier, J. L.; Guyot, A.; Bourgeat-Lami, E. *J Colloid Interface Sci* 2002, 250, 82.
12. Barthet, C.; Hickey, A. J.; Cairns, D. B.; Armes, S. P. *Adv Mater* 1999, 11, 408.
13. Percy, M. J.; Michailidou, V.; Armes, S. P. *Langmuir* 2001, 17, 4770.
14. Agarwal, G. K.; Titman, J. J.; Percy, M. J.; Armes, S. P. *J Phys Chem B* 2003, 107, 12947.
15. Amalvy, J. I.; Percy, M. J.; Armes, S. P.; Wiese, H. *Langmuir* 2001, 17, 4770.
16. Han, M. G.; Armes, S. P. *Langmuir* 2003, 19, 4523.
17. Percy, M. J.; Barthet, C.; Lobb, J. C.; Khan, M. A.; Lascelles, S. F.; Vamvakaki, M.; Armes, S. P. *Langmuir* 2000, 16, 6913.
18. Chen, M.; Wu, L.; Zhou, S.; You, B. *Macromolecules* 2004, 37, 9613.
19. Stöber, W.; Fink, A.; Bohn, E. *J Colloid Interface Sci* 1968, 26, 62.
20. Zeng, Z.; Yu, J.; Guo, Z. X. *J Polym Sci Part A: Polym Chem* 2005, 43, 2835.
21. Zeng, Z.; Yu, J.; Guo, Z. X. *J Polym Sci Part A: Polym Chem* 2004, 42, 2253.
22. Percy, M. J.; Michailidou, V.; Armes, S. P.; Perruchot, C.; Greaves, S. J.; Watts, J. F. *Langmuir* 2003, 19, 2072.
23. Ottewill, R. H.; Schofield, A. B.; Waters, J. A.; Williams, N. St. *J Colloid Polym Sci* 1997, 275, 274.
24. Goodwin, J. W.; Ottewill, R. H.; Pelton, R. *Colloid Polym Sci* 1979, 257, 61.
25. Hajji, P.; David, L.; Gerard, J. F.; Pascault, J. P.; Vigier, G. *J Polym Sci Part B: Polym Phys* 1999, 37, 3172.
26. Manring, L. E. *Macromolecules* 1989, 22, 2673.
27. Elliott, J.; Hamerton, I.; Hay, J. N.; Shaw, S. J. *Polymer* 2003, 44, 3775.